

3. S. J. Baker and E. P. Reddy, *Oncogene* **12**, 1 (1996); M. Tewary and V. M. Dixit, *Curr. Opin. Genet. Dev.* **6**, 39 (1996).
4. H. Hsu, J. Xiong, D. V. Goeddel, *Cell* **81**, 495 (1995).
5. H. Hsu, H. B. Shu, M. G. Pan, D. V. Goeddel, *ibid.* **84**, 299 (1996).
6. M. P. Boldin et al., *J. Biol. Chem.* **270**, 7795 (1995); A. M. Chinnaiyan, K. O'Rourke, M. Tewari, V. M. Dixit, *Cell* **81**, 505 (1995); A. M. Chinnaiyan et al., *J. Biol. Chem.* **271**, 4961 (1996).
7. M. Rothe, S. C. Wong, W. J. Henzel, D. V. Goeddel, *Cell* **78**, 681 (1994).
8. H. M. Hu, K. O'Rourke, M. S. Boguski, V. M. Dixit, *J. Biol. Chem.* **269**, 30069 (1994); G. Mosialos et al., *Cell* **80**, 389 (1995); T. Sato, S. Irie, J. C. Reed, *FEBS Lett.* **358**, 113 (1995); G. Cheng et al., *Science* **267**, 1494 (1995); C. H. Regnier et al., *J. Biol. Chem.* **270**, 25715 (1995); H. Nakano et al., *ibid.* **271**, 14661 (1996); Z. Cao, J. Xiong, M. Takeuchi, T. Kurama, D. V. Goeddel, *Nature* **383**, 443 (1996).
9. M. Rothe, V. Sarma, V. M. Dixit, D. V. Goeddel, *Science* **269**, 1424 (1995).
10. B. Z. Stanger, P. Leder, T. H. Lee, E. Kim, B. Seed, *Cell* **81**, 513 (1995); H. Hsu, J. Huang, H. B. Shi, V. Baichwal, D. V. Goeddel, *Immunity* **4**, 387 (1996).
11. V. Adler, A. Polotskaya, F. Wagner, A. S. Kraft, *J. Biol. Chem.* **267**, 17001 (1992); M. Hibi, A. Lin, T. Smeal, A. Minden, M. Karin, *Genes Dev.* **7**, 2135 (1993); J. M. Kyriakis et al., *Nature* **369**, 156 (1994); B. Derjard et al., *Cell* **76**, 1025 (1994).
12. Z. Xia, M. Dickens, J. Raingeaud, R. J. Davis, M. E. Greenberg, *Science* **270**, 1326 (1995); S. Estus et al., *J. Cell Biol.* **127**, 1717 (1994); J. Ham et al., *Neuron* **14**, 927 (1995).
13. M. Verheji et al., *Nature* **380**, 75 (1996); B. W. Zanke et al., *Curr. Biol.* **6**, 606 (1996).
14. HA-p46SAPK γ -pCDNA3 is a cytomegalovirus (CMV) promoter-based expression vector encoding a hemagglutinin (HA)-tagged version of a 46-kD splice variant of SAPK γ (17). TRAF expression vectors have been described (5, 9). 293 cells were transfected by calcium phosphate coprecipitation with 8 μ g of plasmid DNA. Forty-eight hours after transfection, cells were lysed in RIPA buffer containing 0.5 mM dithiothreitol (DTT), 20 mM β -glycerophosphate, 1 mM sodium orthovanadate, 10 mM sodium fluoride, 1 mM phenylmethylsulfonyl fluoride, leupeptin (20 μ g/ml), and aprotinin (20 μ g/ml). Lysates were cleared by centrifugation, and protein concentration was measured by use of a commercial Bradford protein assay (Promega). Equal amounts of each lysate (usually 500 μ g) were incubated on ice with 2 μ g of antibody to HA (12CA5, Boehringer) for 2 hours. Immune complexes were collected by protein A-agarose for 25 min, washed three times with RIPA buffer containing 20 mM β -glycerophosphate, 1 mM sodium orthovanadate, and 0.5 mM DTT, and then washed once with kinase reaction buffer (KRB) [20 mM Hepes (pH 7.5), 20 mM MgCl₂, 20 mM β -glycerophosphate, 2 mM DTT, 100 μ M sodium orthovanadate, 0.5 mM sodium fluoride]. Samples were finally resuspended with 40 μ l of KRB containing 20 μ M adenosine 5'-triphosphate (ATP), 2.5 μ Ci of [γ -³²P]ATP, and 2 μ g of GST-c-Jun(1-141) and incubated at 30°C for 20 min. Reactions were stopped by addition of 3 \times Laemmli sample buffer; samples were boiled and loaded on 12.5% SDS-polyacrylamide gels. After fixing and drying, gels were autoradiographed at -70°C. Radioactivity was quantitated with a PhosphorImager. The amount of HA-SAPK γ in each sample was analyzed by protein immunoblot on immunoprecipitates of 150- μ g samples. Only experiments with comparable amounts of HA-SAPK γ in each sample were taken into consideration.
15. N. Yamauchi et al., *Cancer Res.* **49**, 1671 (1989); R. J. Zimmermann, A. Chan, S. A. Leadon, *ibid.*, p. 1644; K. Schulze-Osthoff et al., *J. Biol. Chem.* **267**, 5317 (1992); K. Schulze-Osthoff, R. Baeyaert, V. Vandevoorde, G. Haegerman, W. Fiers, *EMBO J.* **12**, 3095 (1993); V. Goossens, J. Grooten, K. DeVos, W. Fiers, *Proc. Natl. Acad. Sci. U.S.A.* **92**, 8115 (1995); P. Mehlen, C. Kretz-Remy, X. Preville, A. P. Arrigo, *EMBO J.* **15**, 2695 (1996).
16. R. Schreck, P. Rieber, P. A. Bauerle, *EMBO J.* **10**, 2247 (1991).
17. V. Adler, A. Schaffer, J. Kim, L. Dolan, Z. Ronai, *J. Biol. Chem.* **270**, 26071 (1995).
18. M. Yan et al., *Nature* **372**, 798 (1994); I. Sanchez et al., *ibid.*, p. 794.
19. G. Natoli et al., unpublished results.
20. M. Muzio et al., *Cell* **85**, 817 (1996); M. P. Boldin, T. M. Goncharov, Y. V. Goltsev, D. Wallach, *ibid.*, p. 803; T. Fernandes-Alnemri et al., *Proc. Natl. Acad. Sci. U.S.A.* **93**, 7464 (1996).
21. A. A. Beg and D. Baltimore, *Science* **274**, 782 (1996); C.-Y. Wang, M. W. Mayo, A. S. Baldwin Jr., *ibid.*, p. 784; D. J. Van Antwerp, S. J. Martin, T. Kafri, D. R. Green, I. M. Verma, *ibid.*, p. 787.
22. M. Hirano et al., *J. Biol. Chem.* **271**, 13234 (1996); C. F. Meyer, X. Wang, C. Chang, D. J. Templeton, T. H. Tan, *ibid.*, p. 8971.
23. I. Berberich et al., *EMBO J.* **14**, 5338 (1996).
24. Z. G. Liu et al., *Cell* **87**, 565 (1996).
25. The β -galactosidase expression vector pCDNA-HislacZ is from Invitrogen. HeLa cells (2.5×10^5 per plate) were seeded on a 35-mm plate. Three hours later cells were transfected by calcium phosphate coprecipitation with 6 μ g of total plasmid DNA. Forty-eight hours after transfection, the cells

were treated with hrTNF- α (1000 IU/ml, Genzyme) with or without ActD (50 ng/ml). After 12 hours the cells were fixed in 3% formaldehyde-buffered saline and stained overnight with phosphate-buffered saline containing X-Gal (0.4 mg/ml), 4 mM potassium ferricyanide, 4 mM potassium ferrocyanide, and 4 mM MgCl₂. Blue cells were visualized by phase contrast microscopy; round blue cells showing intense blue staining and loss of adherence were considered as apoptotic. Results are expressed as the percentage of apoptotic blue cells among the total number of blue cells counted.

26. We thank D. V. Goeddel (Tularik, South San Francisco) for mTRAF1-pRK, mTRAF2-pRK, mTRAF2(87-501)-pRK, mFADD(80-205)-pRK, and mTRADD-pRK and for critically reading the manuscript. M. Karin is gratefully acknowledged for providing GST-Jun(1-223) (Ser^{63,73}→Ala). Supported by the Associazione Italiana Ricerca sul Cancro (AIRC), by the Consiglio Nazionale delle Ricerche (ACRO Project), and by Fondazione Andrea Cesalpino.

29 August 1996; accepted 26 November 1996

Regulation of Cell Cycle Synchronization by *decapentaplegic* During *Drosophila* Eye Development

Andrea Penton, Scott B. Selleck, F. Michael Hoffmann*

In the developing *Drosophila* eye, differentiation is coordinated with synchronization by progression through the cell cycle. Signaling mediated by the transforming growth factor- β -related gene *decapentaplegic* (*dpp*) was required for the synchronization of the cell cycle but not for cell fate specification. DPP may affect cell cycle synchronization by promoting cell cycle progression through the G₂-M phases. This synchronization is critical for the precise assembly of the eye.

The *Drosophila* eye has served as a model system for examining the molecular mechanisms that govern the patterning and assembly of a complex tissue. The adult eye develops from an epithelial monolayer known as the eye imaginal disc. Differentiation begins in the posterior end of the disc and progresses anteriorly, marked by an indentation in the disc epithelium called the morphogenetic furrow (MF). Within the MF, unpatterned cells are induced to differentiate into the highly ordered array of retinal cells and nonneural accessory cells that produce the 750 ommatidia of the adult eye (1, 2). Differentiated cells posterior to the MF express the signaling molecule hedgehog (HH), which directs the anterior advancement of the furrow (3, 4) and induces the expression of DPP within the furrow. DPP mediates cell fate determination in the developing wing and leg in

response to HH (5, 6).

During the initial stages of sensory unit assembly in the MF, precursor cells exhibit synchronization of the cell division cycle (2, 7). Anterior to the MF, cells divide randomly, but just ahead and within the MF, cell divisions occur more coordinately. The first evidence of cell cycle synchronization is increased amounts of cyclin B (8), a mitotic cyclin required for entry into mitosis (9). As cells enter late G₂, cyclin B levels peak and cyclin B then degrades at the metaphase-anaphase transition in mitosis. Loss of cyclin B and the appearance of mitotic figures mark coordination in the M phase (Fig. 1, A through C). After completion of mitosis, cells arrest in G₁ in the MF and transcription of *dpp* is activated (Fig. 1C).

Cells respond to DPP through two type I receptors, *thick veins* (*tkv*) or *saxophone* (*sax*), and a type II receptor, *punt* (*put*) (10). Responses to DPP are also attenuated by mutations in the putative transcription factor *schnurri* (*shn*) (11). We examined whether DPP was necessary for cell fate specification or cell cycle synchronization by determining whether cells defective for *tkv*, *sax*, or *shn* showed abnormalities in cell division or dif-

A. Penton and F. M. Hoffmann, McArdle Laboratory for Cancer Research and Laboratory of Genetics, University of Wisconsin Medical School, Madison, WI 53706, USA. S. B. Selleck, Arizona Research Laboratories Division of Neurobiology and Department of Molecular and Cellular Biology, University of Arizona, Tucson, AZ 85721, USA.

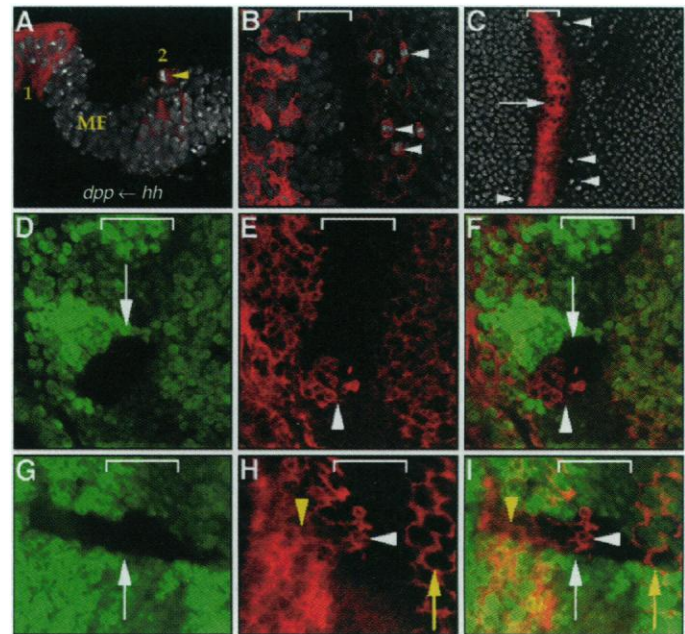
*To whom correspondence should be addressed.

ferentiation. Clones mutant for a null allele of *tkv* that were anterior or posterior to the furrow had amounts of cyclin B that were indistinguishable from those in surrounding normal cells (Fig. 1, G through I). In contrast, *tkv* clones that spanned the MF maintained cyclin B expression in the anterior part of the furrow even though the surrounding cells arrested in G₁ had no detectable cyclin B (Fig. 1, D through I). Clones defective for *sax* and *shn* also showed disruption of cyclin B expression when the clone encompassed the anterior half of the furrow (Fig. 2, A through F). Clones spanning the MF reveal that cyclin B was finally lost in the posterior region of the furrow, despite the absence of DPP signaling. These clones had condensed chromosomes indicative of early stages in mitosis at the interface between the cyclin B-expressing and nonexpressing cells (Fig. 3, A and B).

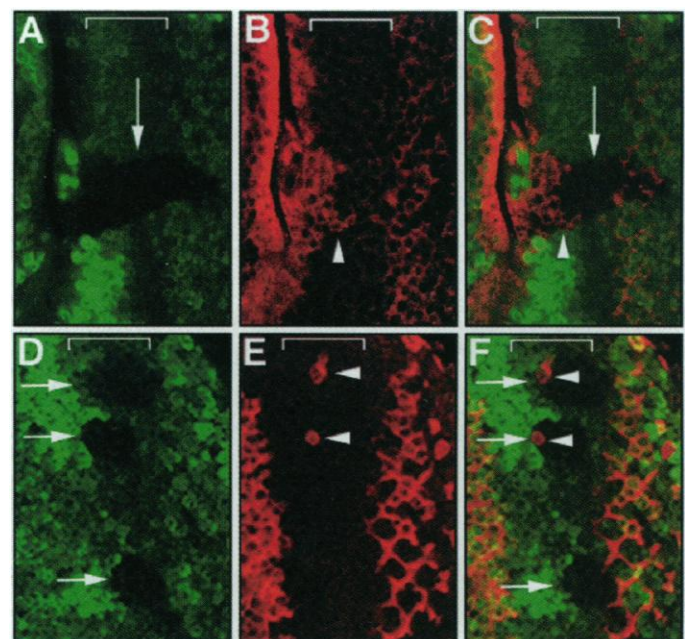
The expression of cyclin B in the mutant cells in the furrow could be interpreted as evidence that DPP inhibits progression through G₁ in the furrow. In this case, cells in the clone might be expected to progress through G₁ and S and reenter G₂, where they would again exhibit cyclin B expression. Failure to arrest in G₁ should produce a clone with patchy expression of cyclin B in the anterior half of the furrow as the asynchronously dividing cells continue through the cell cycle. However, cyclin B expression was continuous in the anterior part of the furrow in *tkv* and *sax* clones in which we examined serial optical sections (Fig. 1, D through I, and Fig. 2, A through C). Furthermore, mitotic figures were not observed in clones in the anterior half of the MF, which suggests that the cells in the clones were not asynchronously progressing through M and into a new cell cycle. The phenotype observed in the clones is similar to defects caused by mutations in the gene *division abnormally delayed (dally)*, which is required for G₂-M progression ahead of the furrow (8). Mutations in *dally* and *dpp* display genetic interactions in development of the eye, antennae, and genitalia, which suggests that *dally* augments *dpp* function (12). Regulation of cell division in the G₂-M transition occurs at several stages in *Drosophila* development, including in embryonic divisions (13), in the wing disc (14), and in the eye disc (4). The behavior of DPP-receptor mutant clones supports a role for DPP in controlling progression through G₂-M as a means of synchronizing the divisions that accompany differentiation in the eye disc.

We next examined whether this defect in synchronization affected patterning or differentiation of cells. For example, mutations in *roughex (rux)* prevent arrest in G₁, cause cells to enter the S phase prematurely, and result in disruptions in cell cycle synchronization and differentiation (7). The assembly of om-

matidia and the synchronization of the cell cycle within the furrow are accompanied by changes in the position of nuclei within the epithelium (1, 15). We examined the position of nuclei in *tkv*, *sax*, and *shn* clones as an



matidia and the synchronization of the cell cycle within the furrow are accompanied by changes in the position of nuclei within the epithelium (1, 15). We examined the position of nuclei in *tkv*, *sax*, and *shn* clones as an



matidia and the synchronization of the cell cycle within the furrow are accompanied by changes in the position of nuclei within the epithelium (1, 15). We examined the position of nuclei in *tkv*, *sax*, and *shn* clones as an

indicator of events that accompany ommatidial assembly. Clones at the anterior edge of the furrow had cells with mislocalized nuclei; they failed to reach the apical surface where mitosis normally takes place in do-

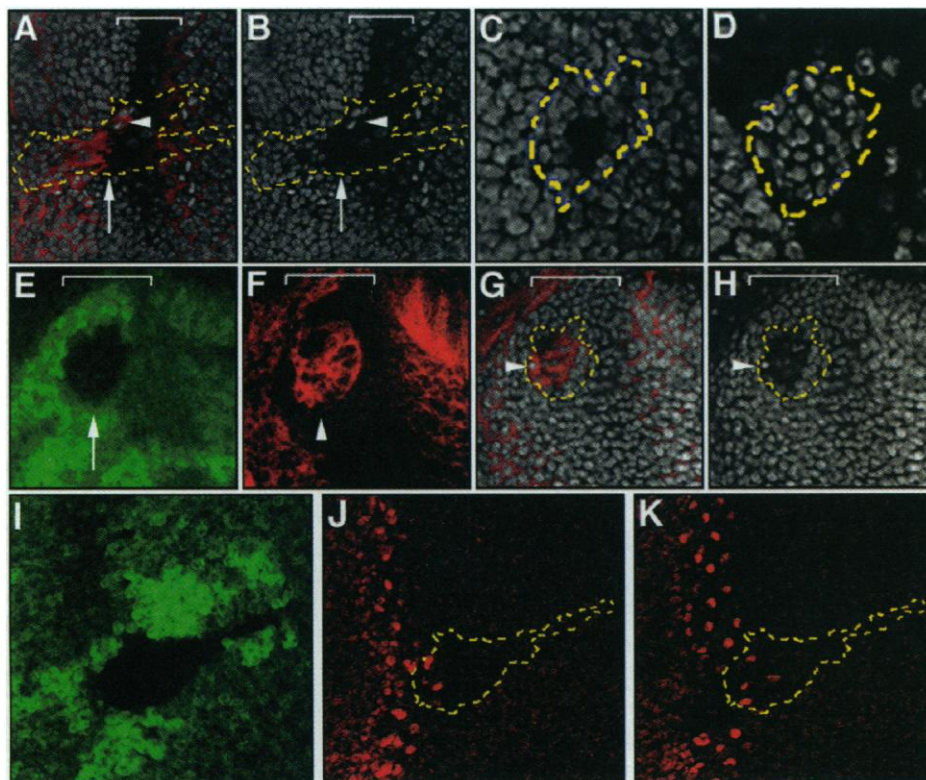
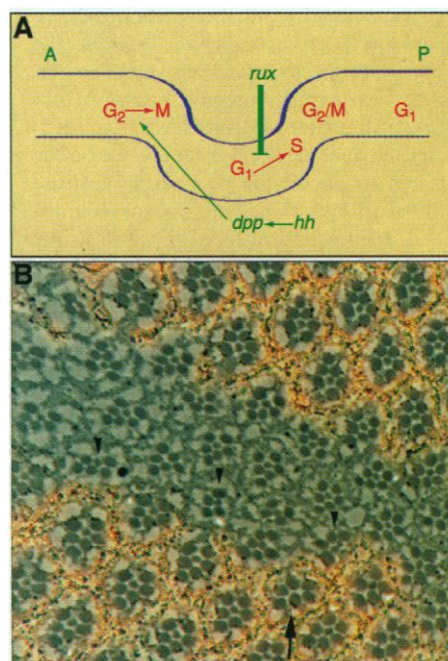


Fig. 3. Mitotic figures and mislocalized nuclei in *tkv* and *shn* clones. Third instar discs were triple-labeled with anti-Myc, anti-cyclin B, and propidium iodide as in Figs. 1 and 2 or with anti-Myc and anti-ATONAL. Clones are indicated by dashed yellow lines in (A) through (D), (G) and (H), and (J) and (K). Nuclei were mislocalized in *tkv* clones as cells began to enter the MF and were not visible in apical sections [arrow in (A) and (B)]. Mitotic figures were discernible in the MF within and slightly posterior to the ectopic cyclin B expression [arrowhead in (A) and (B)]. In *tkv* clones that were posterior to the MF, nuclei were underrepresented in apical sections (C) and overrepresented in basal sections (D). In *shn* clones [arrowheads in (F) and (G)], condensed mitotic chromosomes were discernible in some regions that expressed ectopic cyclin B [arrowheads in (F) and (G)], but most of the remaining nuclei were not visible in apical focal planes [(G) and (H)]. In *tkv* clones (I), *atonal* expression was still present in the presumptive R8 cell (J and K), although apical sections revealed that the nuclei were mislocalized.

Fig. 4. Defects in cell cycle progression and ommatidial assembly caused by lack of DPP signaling. (A) *hh* is expressed in differentiated cells and activates *dpp* transcription in the MF. DPP may diffuse anteriorly and induce cells to enter M ahead of the furrow, possibly by modulating the transcription or activity of a gene involved in G₂-M progression. *rux* prevents cells in G₁ from entering the S phase prematurely (7). (B) Tangential section of an adult eye that contained a *tkv* clone, identified by the lack of pigment cells (19). Normal ommatidia have eight photoreceptor cells, which contain rhabdomeres or rhodopsin-rich apical surfaces, seven of which are visible in each cluster in this section. The clone occurs in the middle of the eye along the dorsal-ventral midline or equator. In the clone, several ommatidia are missing photoreceptor cells (arrowheads). One ommatidia that consists of mostly wild-type tissue also contains abnormalities (arrow).



main 1 (Fig. 3, A and B). Nuclei were also mislocalized when the clone was within the MF and posterior to it (Fig. 3, C through H). Nuclei were underrepresented in apical sections where mitotic figures are normally present (Fig. 3, A through C and G and H) and were overrepresented in basal sections (Fig. 3D). Although nuclei were mislocalized in these clones, cell fate specification was mostly unaffected, as revealed by the expression of the HH-inducible gene *atonal*, a proneural gene required for retinal precursor cell 8 (R8) determination (Fig. 3, I through K) (16), and of the antigen recognized by monoclonal antibody 22C10 (17). Because *atonal* expression was maintained in *tkv* clones, *hh* must not act through *dpp* to induce its expression, and thus *dpp* only mediates a subset of *hh* functions in the MF (Fig. 4A). Tangential sections through adult eyes confirmed that some ommatidia were disorganized in *tkv* clones and lacked the full number of photoreceptor cells (Fig. 4B). Therefore, DPP signaling in the MF appears to be required for cell cycle synchronization and the assembly of ommatidia but not for the specification of cell fate.

REFERENCES AND NOTES

1. D. F. Ready, T. E. Hanson, S. Benzer, *Dev. Biol.* **53**, 217 (1976); A. Tomlinson, *Development* **104**, 183 (1988); T. Wolff and D. F. Ready, in *The Development of Drosophila melanogaster*, M. Bate and A. Martinez Arias, Eds. (Cold Spring Harbor Laboratory Press, Cold Spring Harbor, NY, 1993), vol. II, pp. 1277-1325.
2. A. Tomlinson, *J. Embryol. Exp. Morphol.* **89**, 313 (1985).
3. U. Heberlein *et al.*, *Cell* **75**, 913 (1993); C. Ma, Y. Zhou, P. A. Beachy, K. Moses, *ibid.*, p. 927.
4. U. Heberlein, C. M. Singh, A. Y. Luk, T. J. Donohoe, *Nature* **373**, 709 (1995).
5. K. Basler and G. Struhl, *ibid.* **368**, 208 (1994); F. J. Diaz-Benjumea, B. Cohen, S. M. Cohen, *ibid.* **372**, 175 (1994).
6. M. Zecca, K. Basler, G. Struhl, *Development* **121**, 2265 (1995).
7. B. J. Thomas *et al.*, *Cell* **77**, 1003 (1994).
8. H. Nakato, T. A. Futch, S. B. Selleck, *Development* **121**, 3687 (1995).
9. J. A. Knoblich and C. F. Lehner, *EMBO J.* **12**, 65 (1993).
10. E. Ruberte, T. Marty, D. Nellen, M. Affolter, K. Basler, *Cell* **80**, 889 (1995); A. Letsou *et al.*, *ibid.*, p. 899.
11. K. Arora *et al.*, *ibid.* **81**, 781 (1995); N. C. Grieder, D. Nellen, R. Burke, K. Basler, M. Affolter, *ibid.*, p. 791; K. Staehli-Hampton, A. S. Laughon, F. M. Hoffmann, *Development* **121**, 3393 (1995).
12. S. M. Jackson, H. Nakato, M. Sugiura, S. B. Selleck, in preparation.
13. B. A. Edgar and P. H. O'Farrell, *Cell* **62**, 469 (1990).
14. M. Milan, S. Campuzano, A. Garcia-Bellido, *Proc. Natl. Acad. Sci. U.S.A.* **93**, 640 (1996).
15. J. A. Fischer-Vize and K. L. Mosley, *Development* **120**, 2609 (1994).
16. A. P. Jarman, E. H. Grell, L. Ackerman, L. Y. Jan, Y. N. Jan, *Nature* **369**, 393 (1994).
17. A. Penton and F. M. Hoffmann, unpublished data.
18. To obtain *tkv* clones, males of the genotype *w, tkv⁵ P[ry(+)]hsp70:neo FRT]40A/In(2LR)Gla bc* were crossed to females of the genotype *y w P[ry(+)]hsp70-flp*, *P[w(+)]hsp70 c-myc=PIM]21C P[PIM]36F P[ry(+)]hsp70:neoFRT]40A*. To obtain *sax* or *shn* clones, males of the genotype *w, P[w(+)]FRT]42B sax⁴/In(2LR)Gla bc* or *w, P[w(+)]FRT]42B shn1B/In(2LR)Gla bc* were crossed to females of the genotype *y w P[ry(+)]hsp70-flp*,

P[w(+m)FRT]42B P[PiM]46F P[PiM]47F. Clones of *tkv*, *sax*, or *shn* mutant cells were generated by flip-mediated recombination (flip is a yeast site-specific recombinase) [T. Xu and G. M. Rubin, *Development* **117**, 1223 (1993)]. Discs were stained with a Myc-specific monoclonal antibody, a rabbit antibody to cyclin B, or a rabbit antibody to ATONAL [S. S. Blair, *ibid.* **115**, 21 (1992); J. A. Williams, J. B. Bell, S. B. Carroll, *Genes Dev.* **5**, 2481 (1991)] with the use of a fluorescein conjugate to visualize the antibody to Myc and a Cy-5 conjugate for the antibody to cyclin B or ATONAL. Discs were labeled with propidium iodide after antibody staining [W. G. Whitfield, C. Gonzalez, G. Maldonado-Codina, D. M. Glover, *EMBO J.* **9**, 2563 (1990)]. Thirteen out of 14 *tkv^s* clones that encompassed the anterior half of the MF, and 2 out of 7 clones in the posterior half, had ectopic cyclin B ex-

pression. Nineteen of 29 *shn1B* clones and 10 of 16 *sax^d* clones had aberrant cyclin B expression in the MF. Cyclin B misexpression was less severe in *shn1B* and *sax^d* clones, particularly if they were near the equator. Six *tkv^s* clones in the MF were examined for their effect on *atonal* expression.

19. Clones of *tkv* in adult eyes were induced as above except that males of the genotype *w, tkv^s P[ry(+)]hsp70:neo FRT]40A/In(2LR)Gla* were crossed to females of the genotype *y w P[ry(+)]hsp70-flip*, *P[w(+)]30C P[ry(+)]hsp70:neoFRT]40A*. Sections of adult eyes were made as described [N. L. Brown, C. A. Sattler, D. R. Markey, S. B. Carroll, *Development* **113**, 1245 (1991)]. Ten clones were scored from six sectioned eyes. Seventy-one ommatidia with some or all retinal cells mutant for *tkv* had a normal configuration of seven retinal cells. Thirteen mutant ommatidia

were defective. The defective ommatidia contained from four to six retinal cells. The identity of the missing cell varied, although the altered shape of the clusters did not always permit the identity of the missing cell or cells to be established.

20. We thank N. Perrimon, V. Twombly, M. Singer, and W. M. Gelbert for fly stocks; S. Blair, Y. Jan, W. Whitfield, and D. Glover for antibodies; the W. M. Keck Foundation Neural Imaging Lab for use of their confocal microscope; J. Hudzinski, A. Kusano, and C. A. Sattler for technical help; and S. B. Carroll, K. Basler, and U. Heberlein for comments on the manuscript. Supported by grants from the NIH National Center for Research Resources to F.M.H. and from the National Cancer Institute. S.B.S. is a fellow of the Alfred P. Sloane Foundation.

22 August 1996; accepted 29 October 1996

Activation of Interferon- γ Inducing Factor Mediated by Interleukin-1 β Converting Enzyme

Yong Gu, Keisuke Kuida, Hiroko Tsutsui, George Ku, Kathy Hsiao, Mark A. Fleming, Nobuki Hayashi, Kazuya Higashino, Haruki Okamura, Kenji Nakanishi, Masashi Kurimoto, Tadao Tanimoto, Richard A. Flavell, Vicki Sato, Matthew W. Harding, David J. Livingston, Michael S.-S. Su*

The interleukin-1 β (IL-1 β) converting enzyme (ICE) processes the inactive IL-1 β precursor to the proinflammatory cytokine. ICE was also shown to cleave the precursor of interferon- γ inducing factor (IGIF) at the authentic processing site with high efficiency, thereby activating IGIF and facilitating its export. Lipopolysaccharide-activated ICE-deficient (ICE^{-/-}) Kupffer cells synthesized the IGIF precursor but failed to process it into the active form. Interferon- γ and IGIF were diminished in the sera of ICE^{-/-} mice exposed to *Propionibacterium acnes* and lipopolysaccharide. The lack of multiple proinflammatory cytokines in ICE^{-/-} mice may account for their protection from septic shock.

ICE is a member of the growing family of ICE-like cysteine proteases (caspases) with a substrate specificity for aspartate (1). ICE (caspase-1) was identified on the basis of its proteolytic activity for cleaving the inactive IL-1 β precursor into the 17-kD mature cytokine (2). ICE-deficient mice are impaired in their production of mature IL-1 β (3), which establishes the physiological role of ICE in the processing and export of IL-1 β . In contrast to IL-1 β -deficient mice (4), ICE^{-/-} mice also have less IL-1 α , tumor necrosis factor- α (TNF- α), and IL-6 and are resistant to septic shock induced by endotoxin (3), which suggests that ICE may have additional functions in the regulation of the immune system.

IGIF, an ~18-kD polypeptide that stimulates production of interferon- γ (IFN- γ) by T cells (5), is synthesized as a polypeptide precursor (proIGIF) devoid of a conventional signal sequence (6). The precursor of IGIF is cleaved after Asp³⁵ (6), which suggests that an aspartate-specific protease may be involved. Two families of proteases with substrate specificity for aspartate have been identified; these include the ICE family of cysteine proteases and granzyme B, a serine protease involved in cytotoxic lymphocyte-mediated cell killing and activation of ICE-like cysteine proteases (7, 8). Therefore, we investigated whether one or more of the ICE-family proteases or granzyme B may be involved in the processing of proIGIF and investigated the role that such a cleavage may have in the function of IGIF.

We first used transient coexpression in COS cells (9) to determine whether proIGIF could be processed by some of the known ICE-family proteases (Fig. 1A). Coexpression of proIGIF with ICE or its homolog TX (caspase-4) (10) resulted in the cleavage of proIGIF into a polypeptide similar in size to the naturally occurring 18-kD IGIF. Single point mutations of the catalytic cysteine res-

idues that inactivate ICE and TX (11) blocked cleavage. Coexpression with CPP32 (caspase-3), a protease involved in programmed cell death (apoptosis) (12), resulted in the cleavage of proIGIF into a ~14-kD polypeptide, whereas CMH-1 (caspase-7), a homolog of CPP32 (13), did not appreciably cleave proIGIF. Thus, ICE and TX could cleave proIGIF into a polypeptide similar to the naturally occurring IGIF.

We examined the cleavage of proIGIF by these proteases in vitro with the use of purified recombinant (His)₆-tagged proIGIF as a substrate (14). ICE cleaved the 24-kD proIGIF into two polypeptides of ~18 and ~6 kD (Fig. 1B). The 18-kD polypeptide comigrated with recombinant mature IGIF upon SDS-polyacrylamide gel electrophoresis (PAGE) and contained the same amino acid residues (Asn-Phe-Gly-Arg-Leu) at its NH₂-terminus as did the naturally occurring murine IGIF, indicating that ICE cleaved proIGIF at the authentic processing site (Asp³⁵-Asn³⁶) (6). This cleavage was specific with a catalytic efficiency (k_{cat}/K_m , where K_m is the Michaelis constant) of $1.4 \times 10^7 \text{ M}^{-1} \text{ s}^{-1}$ ($K_m = 0.6 \pm 0.1 \mu\text{M}$; $k_{cat} = 8.6 \pm 0.3 \text{ s}^{-1}$) (15) and was inhibited by the specific ICE inhibitors Ac-Tyr-Val-Ala-Asp-aldehyde (2) and Cbz-Val-Ala-Asp-[(2,6-dichlorobenzoyl)oxyl]methyl ketone (16). Recombinant (His)₆-tagged human proIGIF was also cleaved by ICE with a similar specificity. Although proIGIF had no detectable IFN- γ -inducing activity, ICE-cleaved proIGIF was active in inducing IFN- γ production in T helper type 1 (T_H1) cells (Fig. 1C) (17). TX also cleaved proIGIF into polypeptides of similar size; however, its catalytic efficiency was about two orders of magnitude lower than that of ICE. In a manner consistent with the observation from the COS cell experiments, CPP32 cleaved proIGIF at a different site (Asp⁶⁹-Ile⁷⁰) and the resulting polypeptides had little IFN- γ -inducing activity, whereas CMH-1 and granzyme B did not cleave proIGIF. Thus, both in COS cells and in vitro, ICE can process the inactive IGIF precursor at the authentic maturation site to generate the biologically active form of IGIF.

Y. Gu, G. Ku, K. Hsiao, M. A. Fleming, V. Sato, M. W. Harding, D. J. Livingston, M. S.-S. Su, Vertex Pharmaceuticals Inc., 130 Waverly Street, Cambridge, MA 02139, USA.

K. Kuida, Tokyo Metropolitan Institute of Medical Science, Tokyo, Japan.

H. Tsutsui, N. Hayashi, K. Higashino, H. Okamura, K. Nakanishi, Hyogo College of Medicine, 1-1, Mukogawacho, Nishinomiya, Japan.

M. Kurimoto and T. Tanimoto, Fujisaki Institute, Hayashibara Biochemical Laboratories, Hayashibara Company Inc., Okayama, Japan.

R. A. Flavell, Howard Hughes Medical Institute, Yale University School of Medicine, New Haven, CT 06510, USA.